Anthropogenic osmium in macroalgae from Tokyo Bay reveals widespread contamination from municipal solid waste

Adam D. Sproson[1,2,*] (ORCHID ID: 0000-0002-1107-3673), David Selby[1,6] (ORCHID ID: 0000-0001-9798-2351), Katsuhiko Suzuki[3] (ORCHID ID: 0000-0003-4266-5046), Tomohiro Oda[4,5] (ORCHID ID: 0000-0002-8328-3020), Junichiro Kuroda[2] (ORCHID ID: 0000-0002-2218-4854)

[1]Department of Earth Sciences, Durham University, Durham, UK
[2]Atmosphere and Ocean Research Institute, The University of Tokyo, Chiba, Japan
[3]Submarine Resources Research Center, JAMSTEC, Yokosuka, Japan
[4]Global Modelling and Assimilation Office, NASA Goddard Space Flight Center, Greenbelt, MD, USA
[5]Goddard Earth Sciences Technology and Research, Universities Space Research Association, Columbia, MD, USA
[6]State Key Laboratory of Geological Processes and Mineral Resources, School of Earth Resources, China University of Geosciences, Wuhan, 430074 Hubei, China
*sproson@aori.u-tokyo.ac.jp

Human activity is influencing the global osmium-cycle, driving the Os isotopic composition ($^{187}Os/^{188}Os$) of the hydrosphere and associated sedimentary material to lower values. Here, we present the Re and Os abundance and isotope systematics of macroalgae, a proxy for seawater, from Tokyo Bay to elucidate the potential sources of anthropogenic Os to the Pacific Ocean. Macroalgae from the Uraga Channel, which connects Tokyo Bay to the Pacific Ocean, record relatively low Os abundances (~10.1 pg/g) and a $^{187}Os/^{188}Os$ (~0.9) indicative of surface ocean seawater. Contrastingly, macroalgae within the Bay closest to central Tokyo record the highest Os abundances (~22.8 pg/g) and lowest $^{187}Os/^{188}Os$ values (~0.47) suggesting contamination from human activity. To determine the source of anthropogenic Os we have developed the first Os emission inventory, based on the East Asian Air Pollutant Emission Grid database (EAGrid2010). The close relationship (R^2 = 0.67, *p*-value = <0.05) between Os inventories and macroalgae data suggests municipal solid waste incinerators (MSWIs) are the dominant source of Os to Tokyo Bay. Projections for Japan estimate $\boxed{26^{+38}_{-18}}$ ng Os/m²/yr is released from MSWI smokestacks leading to a concentration in precipitation of $\boxed{26^{+38}_{-18}}$ fg/g, identifying MSWIs as a major contributor of anthropogenic Os to the hydrological cycle.

Introduction

The high Re/Os ratios and average age (ca. 2 Gyr) of the upper continental crust has led to appreciable levels of radiogenic ^{187}Os, from the β-decay of ^{187}Re, relative to more recent mantle derived rocks, generating a wide range in the $^{187}Os/^{188}Os$ values of natural reservoirs (Fig. 1). This has allowed the application of the Re-Os isotope system to trace a range of Earth system processes, from the weathering of continental rocks to the timing of bolide impacts, through geological time[1, 2]. Although geologically recent, accelerated mining, fossil fuel combustion and catalytic converter use since the latter part of the 20th century[3, 4] has led the present-day flux of natural Re and Os to be exceeded by the anthropogenic flux[5, 6], impacting the global Os budget[7].

The mining, smelting and use of unradiogenic mantle-derived, base-metal sulphide[8-10], PGE sulphide[11] and chromium ores[12] and the combustion of radiogenic fossil fuels[13-16], has led to the detection of anthropogenic Os in estuaries[17, 18], coastal sediments[19, 20], lakes[21] and precipitation[7] (Fig. 1). Point sources of anthropogenic Os include sewage outflow[17-20, 22] incinerators[17, 18, 23] and smelters[24-26], whereas automobile catalytic converter exhaust in densely populated regions can impart a significant regional influence[21, 27, 28]. On a global scale, the refining of PGE ores, coupled to the widespread use of catalytic converters, has driven the $^{187}Os/^{188}Os$ of precipitation and oceanic surface waters to more unradiogenic values[7]. Osmium isotopes can therefore be utilised as a powerful tracer of human influence on the hydrological cycle "similar to Pb from leaded gasoline usage before 1978 or tritium from atmospheric atomic bomb testing in the early 1960s"[7].

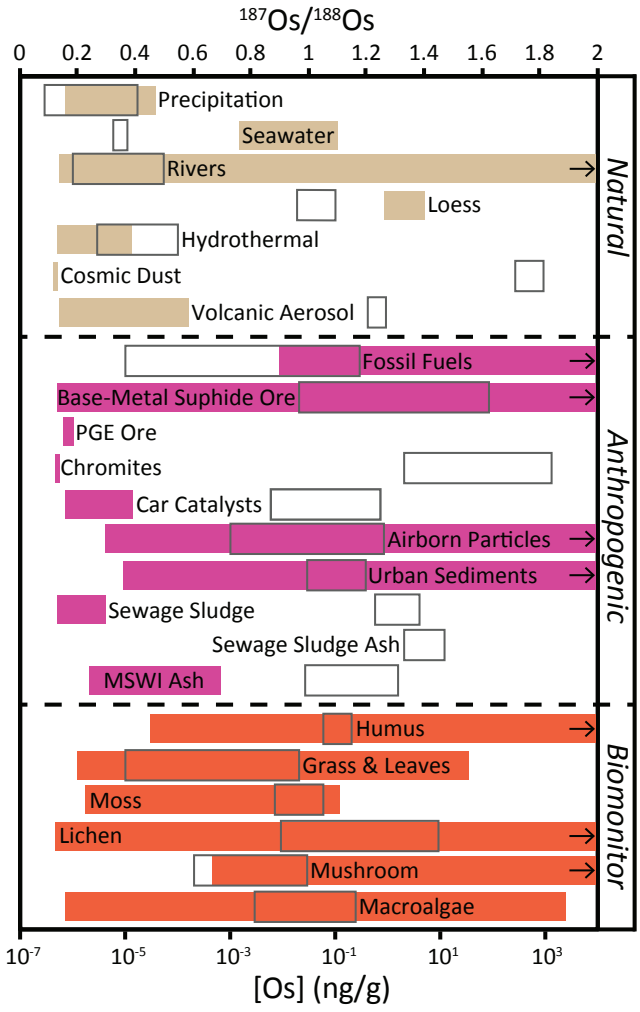

Fig. 1. The Os abundance (open boxes) and isotopic composition (filled squares) of natural sources (tan), anthropogenic sources (pink) and biomonitors (orange), adapted from Chen *et al.*[7] and Funari *et al.*[23]. Black arrows are used when the isotopic composition exceeds the confines of the axes. Data references are as follows: precipitation[7, 29, 30]; seawater[7, 31-35]; rivers[1, 29, 30, 36]; loess[19, 37], hydrothermal[1], cosmic dust[32, 38], volcanic aerosols[39, 40]; fossil fuels[13-16]; base-metal sulphide ores[8-10, 24]; PGE ore[11]; chromite[12, 26]; car catalyst[27]; airborne particles[3]; urban sediments[21, 41]; sewage sludge[18-20]; sewage sludge ash[42]; humus, grass and leaves, moss and mushrooms[43]; lichen[24, 26]; and, macroalgae[44-47] (this study).

Biomonitoring the Os cycle. Despite the aforementioned potential, routine analysis of Os in water samples has been hampered by its ultra-low concentration and multiple oxidation states[48]. Biomonitors provide significant advantages when integrating seasonal and/or spatial variations and when economic considerations prevent the use of complex and expensive methods[49]. Ideal biomonitors should be abundant, sedentary, long lived, available year-round and accumulate the relevant element to a sufficient abundance for analysis[50, 51]. Terrestrial biomonitors of airborne Os include leaves, mushrooms, mosses and lichens[43] which have been utilised to trace pollution sourced from smelters[24, 26] (Fig. 1). The common macroalgae (seaweed) species *Fucus vesiculosus* concentrates Re and Os from seawater, without fractionating the various isotopes of Os, confirming the viable use of macroalgae as a marine biomonitor of the Os cycle[47, 52]. Recent applications include a tracer of continental weathering provenance in Greenland[45] and Iceland[44] and anthropogenic sources to the Forth estuary, Scotland[46] (Fig. 1).

This study presents Re-Os abundance and isotope data for macroalgae from Tokyo Bay (Japan), a body of water adjacent to the world's largest megacity, to access the potential of macroalgae as a biomonitor of a variety of anthropogenic Os sources. When combined with a newly developed Os emission inventory, macroalgae analysis from this study suggests the widespread emission of anthropogenic Os from the incineration of municipal solid waste is altering the Re-Os isotope composition of Japan towards that of a juvenile igneous terrain. After PGE ore refining, MSWIs are a major contributor of anthropogenic Os to the global Os cycle, helping to drive the $^{187}Os/^{188}Os$ of surface seawater and precipitation to low $^{187}Os/^{188}Os$ values.

Materials and Methods

Sample setting, collection and preparation. The Tokyo Bay catchment basin is one of the most densely populated and industrialized in the world. The city of Tokyo and the surrounding metropolitan area is home to more than 29 million people, representing 23 % of the total population of Japan within 2 % of the gross area, associated with a wide range of agricultural, industrial and municipal activities[53, 54]. With respect to Os, potential anthropogenic point sources include the 29 sewage treatment plants, 18 municipal solid waste incinerators and 7 oil refineries surrounding the coast of the bay[55]. These sources, along with a more regional source of Os associated with the widespread use of catalytic converters, are deposited in Tokyo Bay either directly from the atmosphere or via freshwater discharge, greater than 90 % of which flows from the Edo, Tsurumi, Ara, Tama and Sumida rivers[53] (Fig. S1). Tokyo Bay is connected to the Pacific Ocean via the Uraga Channel with the Boso Peninsula to the east and Miura Peninsula to the west (Fig. S1).

Macroalgae from the coast of Tokyo Bay and the Uraga Channel were sampled at fifteen locations between July and September, 2015 (Fig. S1). Three green (*Mostroma nitidum*, *Urospora penicilliformis*, *Undaria pinnatifidia*), two brown (*Hizikia fusiformis*, *Dictyopteris undulata Holmes*) and one red (*Gloiopeltis complanata*) macroalgae species were used for analysis (Table S1). Data presented in Table S1 represents the analysis of an individual macroalgae for each location. Macroalgae sampling procedures follow Sproson *et al.*[44]. In Brief, macroalgae were washed thoroughly using tap water and then deionized (Milli-Q™) water to remove any attached sediment and salt. Any remaining attached particulates were removed from subsamples using tissue before being rinsed with MQ water again.

Subsamples were stored in zip-lock plastic bags after being dried for 12 hr at 60 °C. Dried macroalgae were crushed/powdered using an agate pestle and mortar prior to analysis.

Re-Os analysis. The Re-Os analysis of macroalgae were carried out in the Durham Geochemistry Centre (Laboratory for Sulfide and Source Rock Geochronology and Geochemistry and Arthur Holmes Laboratory). The technique for chemical separation of Re and Os from macroalgae is reported by Racionero-Gómez *et al.*[47]. In short, ~200 mg of powdered macroalgae was introduced into a Carius tube. A known amount of a mixed ^{185}Re + ^{190}Os tracer solution, 11 N HCl (3 ml) and 15.5 N HNO_3 (6 ml) were added before heating in an oven for 24 hr at 220 °C. The ^{185}Re and ^{190}Os abundances in the mixed spike were calibrated using Re and Os standard solutions made from 99.9 % pure Re metal and ammonium hexachlorosmate, with its Os content determined gravimetrically[56]. Calibrations of the ^{185}Re and ^{190}Os abundance agree to 0.08 and 0.16%, respectively[57]. The Os was isolated from the acid medium using $CHCl_3$ solvent extraction and then back extracted into HBr. The Os was further purified using a CrO_3-H_2SO_4-HBr microdistillation[58, 59]. The remaining Re-bearing acid medium was evaporated to dryness at 80 °C, with the Re isolated and purified using both NaOH-acetone solvent extraction and HNO_3-HCl anion chromatography[60].

Mass Spectrometry. The purified Os and Re fractions were loaded onto Pt and Ni filaments, respectively, and measured using NTIMS[61, 62] on a Thermo Scientific TRITON mass spectrometer using an electron multiplier in dynamic mode and Faraday collectors in static mode, respectively. The Os and Re abundances and isotope compositions are presented with 2 SE (standard error) absolute uncertainties, which include full error propagation of uncertainties in the sample and spike weights, blank, spike calibrations and mass spectrometer measurements (Table S1). Full analytical blank values for the macroalgae analysis are the same as in Sproson *et al.*[44] at 0.13 ± 0.13 pg for Os, with a $^{187}Os/^{188}Os$ composition of 0.61 ± 0.34, and 10.9 ± 5.9 pg for Re (1 SD, n = 4). Analytical blanks were calculated by carrying out the full chemical procedure alongside samples. Macroalgae sample blanks were variable and corrected using the individual blank values for each sample run. To monitor the long-term reproducibility of mass spectrometer measurements, Os (DROsS) and Re reference solutions were analyzed. A 50 pg DROsS solution gave an $^{187}Os/^{188}Os$ ratio of 0.16111 ± 0.0008 (2 SD, n = 8), which is in agreement with reported value for the DROsS reference solution[63]. The 125 pg Re solution yields an average $^{185}Re/^{187}Re$ ratio of 0.5987 ± 0.0023 (2 SD, n = 8), which is in agreement with published values[60]. Following Ownsworth *et al.*[46], the 'in house' macroalgae reference material, RMKB, was analysed to test the reproducibility of macroalgae Re-Os measurements (Table S2). Analysis of RMKB respectively recorded a Re abundance, Os abundance, $^{187}Os/^{188}Os$ and $^{187}Re/^{188}Os$ of 28.1 ± 0.8 ng/g, 7.5 ± 0.1 pg/g, 0.809 ± 0.003 and 19,759 ± 910 (2SD, n = 4) which is in agreement with previously reported values[46].

Osmium emission inventory. The emission intensity of anthropogenic sources was obtained from the EAGrid2010 database[64], a widely used emission inventory compiled for air quality models of Japan. The inventory has a temporal and spatial resolution of 1 month and 1 km, respectively. The average annual CO_2 emission inventory for 2011 was increased by 4.9 % to represent values for the year 2015 [65]. Emissions for relevant sources in the Tokyo Bay area,

such as motor vehicle exhaust and MSWI, were then converted to Os emission intensities as described below.

Total gas (CO, CO_2, NH_3, NMVOC, NO_x and SO_x) and particulates (PM_{10} and $PM_{2.5}$) for small (injection height < 25 m), medium (25 m <= injection height < 100 m) and large (injection height >= 100 m) waste incinerators were converted to volatile OsO_4 emissions using an average value of 0.31 ng Os per g of gas and particulates, with an average $^{187}Os/^{188}Os$ of 0.44, estimated for a medium size MSWI[23]. The EAGrid2010 point source emission inventories are not considered to be subject to spatial modelling uncertainty[65]. We therefore based uncertainty estimates on the range of Os abundances from the literature, using a value of 0.09 and 0.77 ng Os per g of gas and particulates to provide the upper and lower levels of MSWI Os emission estimates, respectively[23].

Motor vehicle exhaust CO_2 was converted to volatile OsO_4 emissions by taking an average estimation of 82.7 ng Os for a catalytic converter[27], and assuming each vehicle in Japan produces 0.67 t CO_2/a, to give 133.6 ng Os/t CO_2 with a $^{187}Os/^{188}Os$ of 0.17. The total Os emissions estimated for vehicle exhaust will be reduced to 7.2 % to represent the percentage of new cars on the road in 2014 and 2015 (5,562,888 new vehicles of 77,188,461 total vehicles)[66], as all Os from a catalytic converter is expected to be lost within the first year of use[27]. Although uncertainties are expected from the EAGrid2010 gridded emission product they are hard to access due to the lack of physical measurements [65, 67, 68]. Thus, gridded vehicle emission inventories are generally provided without uncertainties. Based on the range of 6 to 228 ng Os for new catalytic converters estimated in the literature[27], a value of 9.7 and 367.7 ng Os/t CO_2 are used to provide the respective upper and lower levels of vehicle Os emission estimates.

Results and Discussion

The Re-Os systematics of macroalgae in Tokyo Bay. Rhenium behaves conservatively during mixing between seawater and freshwater, decreasing with salinity[44, 69]. Osmium, on the other hand, behaves nonconservatively, displaying Os removal at low salinity, in temperate and polar regions[34, 70], and high salinity, in the tropics[17, 71]. Riverine Os abundance is highly variable (average = 9.1 pg/kg; range = 4.6 to 52.1 pg/kg)[29, 36] relative to more constant oceanic values (~10 pg/kg)[31, 32, 35] leading to an increase or decrease with salinity in estuaries dependent on the concentration of the riverine endmember[17, 34, 70, 71]. This behaviour generally leads to high oceanic $^{187}Re/^{188}Os$ values (4270) relative to riverine values (227)[1].

The Re and Os abundance of macroalgae has be shown to have no significant relationship with macroalgae species[44], supported by an ANOVA conducted here between macroalgae species (See Text S1). Instead the Re and Os abundance of macroalgae increases with that of the seawater in which it lives[47, 52], displaying a similar relationship with salinity as direct water measurements, both in terms of abundance and $^{187}Re/^{188}Os$ ratios[44]. This relationship is recorded in the Re and Os abundance of macroalgae studied here (Table S1), which respectively decrease from 2.9 ng/g and 10.1 pg/g on the Boso Peninsula to 0.05 ng/g and 3.6 pg/g on the Miura Peninsula (Fig. 2a and 2b). Rhenium abundance remains relatively low at ~0.4 ng/g along the west coast of Tokyo Bay under strong freshwater influence from the major rivers running through the Tokyo metropolitan area but increases again at places (Sample location 2, 3, 5 and 6) along the northeast coast of Tokyo Bay to ~2.8 ng/g,

suggesting an additional source of Re at these locations (Fig. 2b). Osmium abundance increases again to ~6.4 pg/g along the north east coast of Tokyo Bay, reaching maximum values of 12.2 to 30.1 pg/g near the Tokyo metropolitan area, suggesting an additional source of Os is emanating from central Tokyo (Fig. 2a). This is reflected in the $^{187}Re/^{188}Os$ of macroalgae, a qualitative indicator of freshwater influence[44], which shows a decrease from ~1310 on the Boso Peninsula to ~73 in Tokyo Bay (Fig. 2c) following a general decrease in salinity from ~34 g/kg at the Miura Peninsula to ~28 g/kg at the head of the bay[72]. Macroalgae from sample location 2, 3, 5 and 6 show elevated $^{187}Re/^{188}Os$ ratios of 640 to 4462 (Fig. 2c) related to the additional source of Re previously discussed (Fig. 2b).

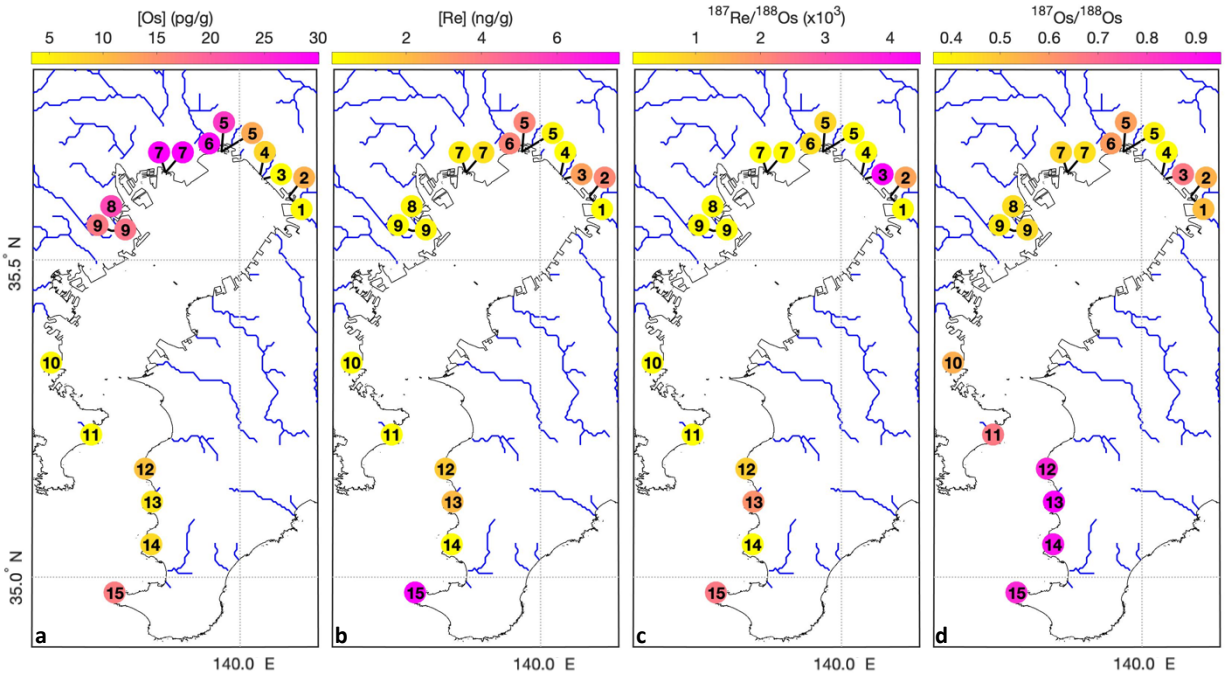

Fig. 2. The spatial distribution of macroalgae Os abundance **(a)**, Re abundance **(b)**, $^{187}Re/^{188}Os$ **(c)** and $^{187}Os/^{188}Os$ **(d)**. The thin black line outlines the Japanese coastline while the thick black lines denote sample locations. Blue lines represent major river systems.

The $^{187}Os/^{188}Os$ composition of macroalgae represents the long-term (months to years) $^{187}Os/^{188}Os$ composition of seawater[44, 47], which in turn reflects the balance between various natural and anthropogenic inputs (Fig. 1), and can be utilised to determine the sources of Os and Re to Tokyo Bay. The $^{187}Os/^{188}Os$ of the floating macroalgae, *Sargassum fluitans* and *S. natans*, from the Gulf of Mexico[45] and the commercially farmed macroalgae, *Laminaria japonica*, from the coast of Hokkaido[46] are indistinguishable from the oceanic value of 1.06 [1]. Macroalgae from the Boso Peninsula have a $^{187}Os/^{188}Os$ value of 0.85 to 0.95 (Fig. 2d) suggesting they are largely influenced by water from the nearby Pacific Ocean (Fig. S1) defined by a relatively radiogenic $^{187}Os/^{188}Os$ of ~1.02 [7, 32].

As seawater becomes mixed with freshwater influx, such as in estuaries, macroalgae begin to take on the $^{187}Os/^{188}Os$ composition of a mixture between these two sources[44]. The natural $^{187}Os/^{188}Os$ composition of rivers generally reflects that of the weathered bedrock within a catchment area, which shows a wide range of values[29, 30] (Fig. 1) from the weathering of highly unradiogenic juvenile basaltic crust ($^{187}Os/^{188}Os$ = 0.12), recorded in macroalgae from Icelandic coastal waters[44], through to the weathering of more radiogenic

old granitic crust ($^{187}Os/^{188}Os$ = 1.4), recorded in macroalgae from the coastal waters of Greenland[45]. Around 71 % of freshwater inputs to Tokyo Bay are fed by the Tsurumi, Ara, Tama and Sumida rivers, which pass through the Tokyo Metropolitan area underlain by Quaternary sedimentary rocks (siltstones, sandstones and conglomerates), sourced in the Kanto Mountains composed of Mesozoic sedimentary rocks (sandstone, mudstone, chert and conglomerates) and Paleozoic metamorphic rocks (metabasalt and schists) belonging to the Sambagawa metamorphic belt[73-75]. Although no Re-Os isotope data has been recorded for this region, stream sediments (Geological Survey of Japan, GSJ, reference material JSd-3) from the Tsukuba and Yamizo mountains, with an underlying geology similar to the Kanto mountains i.e. Mesozoic sandstone and mudstone but with some Miocene andesite and basalt, to the north of Tokyo Bay record a $^{187}Os/^{188}Os$ of 1.07 ± 0.07 [76]. This is consistent with the $^{187}Os/^{188}Os$ values of other rivers draining sedimentary and igneous terrains, such as the Hong He, Chang Jiang, Yukon and the Mississippi, which are defined by radiogenic compositions equal to or greater than that of the eroding upper continental crust (1.05 ± 0.23), reaching values as high as ~2.3 in the Xijiang river[1, 37].

We would therefore expect the $^{187}Os/^{188}Os$ of macroalgae from the Uraga Channel and Tokyo Bay to represent a mixed composition between seawater and a more radiogenic natural freshwater endmember. However, the $^{187}Os/^{188}Os$ of macroalgae studied here decreases from radiogenic values along the Boso Peninsula to more unradiogenic values of 0.55 to 0.67 on the Miura Peninsula, reaching values of ~0.49 (0.36 to 0.67) in Tokyo Bay (Fig. 2d). This suggests an additional source of unradiogenic Os to Tokyo Bay. Natural unradiogenic Os inputs relevant to Japan include volcanism and the weathering of mafic material. The nearest regions of relevance to Tokyo Bay are the Izu Peninsula, to the southwest of Tokyo Bay, and the Akagi and Asama volcanoes, to the northwest of Tokyo Bay, which primarily consist of Quaternary to Neogene andesite and pyroclastic rocks[73, 75, 77]. The $^{187}Os/^{188}Os$ of andesite from the Goshikidai sanukitoid (GSJ reference material JA-2) is ~0.21 ± 0.03 representing a potential natural unradiogenic endmember to Japanese catchment areas[78]. However, the Izu peninsula catchment area drains directly into the Pacific Ocean and the Akagi and Asama volcanoes partly source the Tone river system which runs through the Kanto plains, bypassing Tokyo Bay, exiting directly to the Pacific Ocean in the east[75, 77]. This suggest natural inputs to Tokyo Bay are likely to be dominated by radiogenic Os from the rivers within the Tokyo Bay catchment area, and an additional source of unnatural Os is needed to drive macroalgae to unradiogenic values.

Anthropogenic sources of Os to Tokyo Bay. Additional anthropogenic sources of Os to Tokyo Bay include the smelting of ores, refinery and use of fossil fuels, the incineration or outfall of solid or medical waste and catalytic converter exhaust (Fig. 1). Although several steelworks occupy the western and eastern coast of Tokyo Bay, the smelting of high-Os base-metal sulphide, PGE or chromite ores is not known to occur within the vicinity of the Kanto Plains[55]. Moreover, although seven oil refineries reside around Tokyo Bay, the $^{187}Os/^{188}Os$ of fossil fuels is highly radiogenic (0.9 to 13.7) and therefore cannot represent the unradiogenic source recorded in macroalgae[13-16]. The large number of MSWIs, hospitals, medical research facilities and vehicles in Tokyo and the surrounding metropolitan areas could potentially contribute to the unradiogenic nature of Os in Tokyo Bay (Fig. 1).

To ascertain the relative contribution and distribution of Os from these sources we have derived Os emission estimates using the EAGrid2010 emission inventory (See materials and methods). This model reveals a substantial emission of anthropogenic Os to the northwest of Tokyo Bay emanating from MSWIs (< $\boxed{84^{+136}_{-56}}$ g Os/km^2), close to central Tokyo (Fig. 3a), and vehicle exhaust (< $\boxed{514^{+1399}_{-476}}$ µg Os/km^2), in central Tokyo and near major highways (Fig. 3b). Exhaust emissions decrease along the Miura Peninsula and the northeast coast of Tokyo Bay, reaching values below $\boxed{50^{+250}_{-45}}$ µg Os/km^2 for much of the Boso Peninsula (Fig. 3b). The distinct $^{187}Os/^{188}Os$ of MSWI ash (0.44) relative to catalytic converters (0.17) leads to a large variation in the $^{187}Os/^{188}Os$ of Os emissions (Fig. 3d). Vehicle exhaust Os emissions are several orders of magnitude lower than MSWIs, leading to a dominance in total Os emissions from MSWIs (Fig. 3c) and a $^{187}Os/^{188}Os$ close to 0.44 within the vicinity of Tokyo Bay (Fig. 3d). Measurements of the used car catalysts standard, SRM-2557, recorded a higher Os concentration (631 to 721 pg/g) than new catalytic converters (6 to 228 pg/g) with a significantly more radiogenic $^{187}Os/^{188}Os$ of 0.38 [27], closer to values recorded in macroalgae from Tokyo Bay, suggesting recycling of more radiogenic Os possibly from the combustion of fossil fuels (Fig. 1). However, even if we assume Os is recycled in all catalytic converters by using 100 % of vehicle emissions, as opposed to 7.2 %, and an Os abundance of 721 pg/g, maximum vehicle Os emissions for Tokyo Bay still only reach 0.04 g Os/km^2, considerably lower than the range estimated for MSWIs (Fig. 3a).

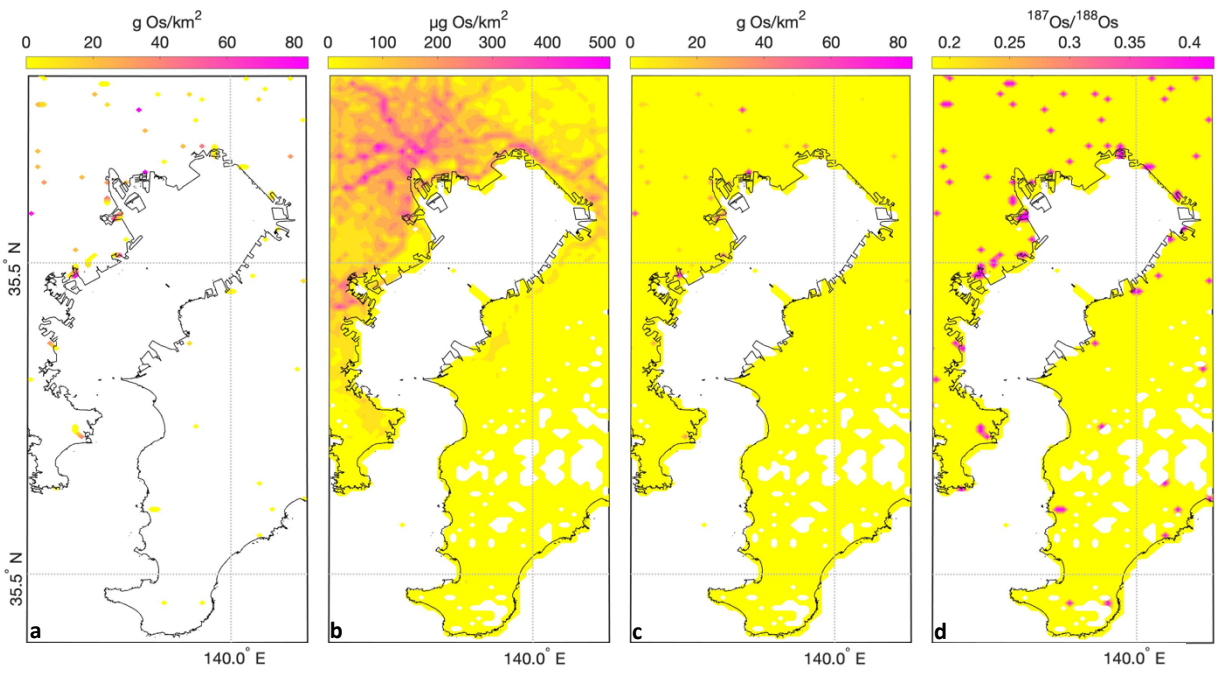

Fig. 3. The spatial distribution of Os emissions from MSWIs **(a)** and vehicle exhaust **(b)** estimated for 2015 from the EAGrid2010 emission inventory. Note that MSWI and vehicle exhaust emissions are displayed with different units. Total combined MSWI and vehicle exhaust emissions **(c)** are shown with their corresponding $^{187}Os/^{188}Os$ isotope ratios **(d)**. See materials and methods for details. The thin black line outlines the Japanese coastline.

Osmium emitted from these sources is likely to be in the form of osmium oxide which is gaseous at temperatures (OsO_4 becomes volatile above 110°C) associated with the operation of waste incinerators and catalytic converters[23, 27]. Gaseous OsO_4 is rapidly

scavenged by dust particles or precipitation where it is deposited in local sediments, estuaries, lakes and seawater[3, 7, 17-21]. Atmospheric deposition of anthropogenic Os has been recorded by terrestrial biomonitors, resulting in highly unradiogenic $^{187}Os/^{188}Os$ compositions[24, 26], while the marine biomonitor, macroalgae, detected relatively unradiogenic freshwater inputs from the industrialised regions of the Firth and Forth estuary[46]. Moreover, when a culture of the macroalgae species, *F. vesiculosus*, is doped with highly unradiogenic Os ($^{187}Os/^{188}Os$ = 0.16), it rapidly takes on the $^{187}Os/^{188}Os$ composition of the culture medium[47]. Macroalgae from Tokyo Bay show the highest Os abundance (Fig. 2a) in the region of highest modelled Os emissions (Fig. 3c), with a similar $^{187}Os/^{188}Os$ of ~0.47 (Fig. 2d) to sediments from the Tama River[41] and Tokyo Bay (GSJ reference material JMS-1)[76] and the modelled emissions of ~0.44 related to MSWI emissions (Fig. 3d). The higher Re abundance, $^{187}Re/^{188}Os$ and $^{187}Os/^{188}Os$ of macroalgae from sample location 5, 6, 3 and 2 suggest an additional source of Re and Os coming from the northeast of Tokyo Bay (Fig. 2). A point source of high terrestrial organic matter and agricultural inputs from the nearby Hanami River[53] would be both high in Re and radiogenic Os[47, 79, 80] potentially leading to higher values in nearby macroalgae.

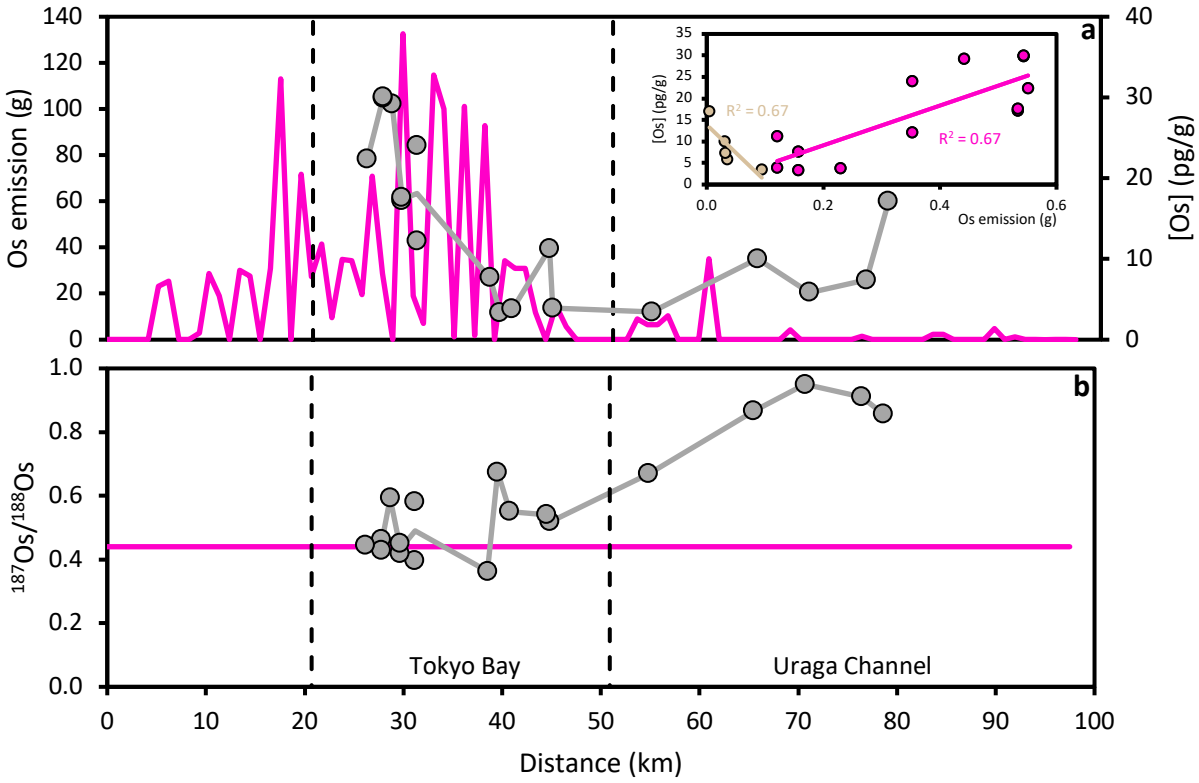

Fig. 4. A northeast to southwest transect of Os abundance **(a)** and Os isotopic composition **(b)**. Average MSWI (pink) Os emissions from Fig. 3 are compared to macroalgae data (grey) presented in Fig. 2. The dashed black line delimits the boundaries between Tokyo Bay and the Uraga Channel. Comparison of average MSWI emissions within a 400 km^2 area of the sample locations and the corresponding Os abundance of macroalgae are displayed in the inset of **a** for Tokyo Bay (pink) and the Uraga Channel (tan). All relationships displayed are significant to $p = < 0.05$.

When plotted along a northwest to southeast transect, macroalgae Os abundance shows a similar relationship to MSWI (R^2 = 0.67, *p*-value = <0.05) Os emission estimates, decreasing from maximum values close to Tokyo City to minimum values along the transition from Tokyo Bay to the Uraga Channel (Fig. 4a). Macroalgae Os abundance then increases along the Uraga Channel which is negatively correlated to MSWI Os emissions (inset of Fig. 4a) suggesting another source of Os to the Uraga channel. This trend is reflected in the $^{187}Os/^{188}Os$ of macroalgae, which increases from values similar to modelled Os emissions (pink line in Fig. 4b) in Tokyo Bay, to more radiogenic values indicative of Pacific Ocean seawater[7, 32] ($^{187}Os/^{188}Os$ = ~1.02) towards the end of the Uraga Channel (Fig. 4b). The increase in Os abundance seaward within the Uraga Channel could be driven by gradual mixing of low Os abundance water from Tokyo Bay and more abundant seawater from the Pacific Ocean, or the removal of Os at high salinity (30 to 34 g/kg)[72] during transition from Tokyo Bay to the Uraga Channel (Fig. 4).

Both the spatial (Figs. 2 and 3) and latitudinal (Fig. 4) distribution of Os abundance and isotopic composition of macroalgae and emission inventories point towards MSWIs as the dominant source of Os to Tokyo Bay. This may be compounded by the addition of Os from sewage sludge outfall, with a higher Os abundance than both catalytic converters and MSWI ash[17-20] (Fig. 1), from 26 sewage treatment plants around Tokyo Bay[55]. This suggests that human activity is influencing the Os isotope systematics of Tokyo Bay, driving the $^{187}Os/^{188}Os$ of macroalgae to unradiogenic compositions.

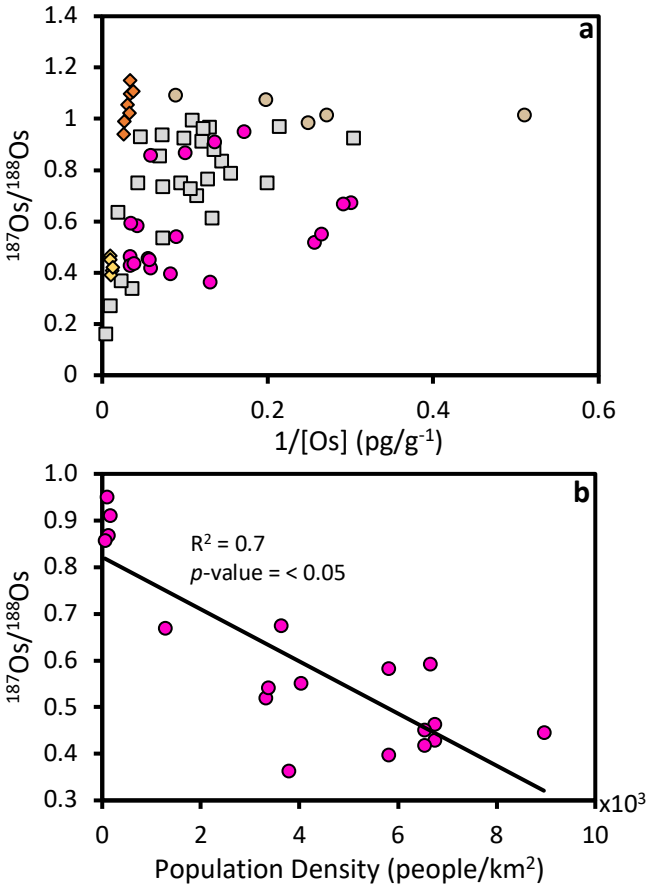

Fig. 5. (a) Osmium isotopic composition ($^{187}Os/^{188}Os$) against the reciprocal of the Os abundance for macroalgae from Tokyo Bay (pink circles; this study), Hokkaido[46] (tan circles)

and Iceland[44] (grey squares) and GSJ reference materials[76] JSd-3 (orange diamonds) and JMS-1 (yellow diamonds). **(b)** The $^{187}Os/^{188}Os$ of macroalgae from Tokyo Bay against the average population density (2015) within a 400 km^2 area of the sample location (See Fig. S1).

The impact of human activity on the global Os cycle. When the $^{187}Os/^{188}Os$ of macroalgae from the pristine waters off the coast of Hokkaido[46] is shown against the reciprocal of the Os abundance they fall along a line delimited by two endmembers: seawater (intermediate [Os], radiogenic $^{187}Os/^{188}Os$) and rivers draining a relatively old (Cretaceous to Quaternary) igneous and sedimentary rocks (low [Os], radiogenic $^{187}Os/^{188}Os$) (tan circles in Fig. 5a). Macroalgae (pink circles in Fig. 5a) and sediments (yellow diamonds in Fig. 5a) from Tokyo Bay deviate from this relationship towards a third endmember (high [Os], unradiogenic $^{187}Os/^{188}Os$) related to MSWI emissions, vehicle exhaust and sewage outfall in areas of high population density (Fig. 5b). Human activity is therefore driving the Os isotope signature of Japan from that of a Paleozoic to Quaternary metamorphic, igneous and sedimentary plain (orange diamonds in Fig. 5a) to that of a juvenile basaltic terrain such as Iceland (grey squares in Fig. 5a).

Despite the sequestration of Os to sediments and removal at low salinities in Tokyo Bay, some anthropogenic Os will be transported via the Uraga Channel to the Pacific Ocean. If we assume that surface waters at the mouth of the Uraga Channel (mix) represent the mixing between anthropogenic Os from Tokyo Bay (anth) and seawater Os from the Pacific Ocean (sw), we can determine the abundance of anthropogenic Os entering the Pacific Ocean using the following equation:

$$[Os]_{anth} = \frac{[Os]_{sw}(^{187}Os/^{188}Os_{sw} - {}^{187}Os/^{188}Os_{mix})}{^{187}Os/^{188}Os_{mix} - {}^{187}Os/^{188}Os_{anth}}$$

Assuming the respective isotopic composition of macroalgae from sample site 15 ($^{187}Os/^{188}Os$ = 0.86) and sample sites 1 to 9 ($^{187}Os/^{188}Os$ = 0.49) represents $^{187}Os/^{187}Os_{mix}$ and $^{187}Os/^{187}Os_{anth}$, and given a respective $[Os]_{sw}$ and $^{187}Os/^{188}Os_{sw}$ of 8.2 fg/g and 1.02 [7], we estimate ~3.6 fg/g of anthropogenic Os ($[Os]_{anth}$) in surface waters at the mouth of the Uraga Channel. Using a flow rate of 8 x 10^9 m^3/yr for surface waters leaving the Uraga Channel[81], this amounts to ~29 g of anthropogenic Os being delivered to the Pacific Ocean from Tokyo Bay per year. Considering that the greater Tokyo metropolitan area represents ~1.2 % of the global population living within the coastal region, this figure could rise to 2.2 kg Os/yr from global MSWI, sewage and catalytic converter use. Chen *et al.*[7] calculated it would take 2,391 kg of anthropogenic Os per year, over the last 30 years, to drive the $^{187}Os/^{188}Os$ of the surface ocean mixed layer from 1.05 to 0.95, suggesting direct runoff of anthropogenic Os to the continental shelf provides an insignificant contribution to the global Os cycle.

The refining of PGE ores has been proposed as the major contributor of anthropogenic Os to the ocean, resulting in the emission of ~2,657 kg of anthropogenic Os to the atmosphere per year and a concentration in precipitation (~9 fg/g) on the same order as measured samples[7]. From Os emission inventories we obtain $\boxed{6^{+10}_{-5}}$ pg Os/m^2/yr and $\boxed{26^{+38}_{-18}}$ ng Os/m^2/yr are distributed across Japan from vehicle exhaust and MSWIs, respectively (Fig. S2). The former falls close to the lower end of the estimated range of 3 to 126 pg Os/m^2/yr for the New York City metropolitan area[27], whereas the latter is similar to previous estimates of 16 to 38 ng

Os/m^2/yr for a medium sized European country[23]. Even if Os is recycled within catalytic converters, creating a maximum estimate of 0.4 ng Os/m^2/yr for vehicle exhaust, the incineration of MSW remains the more dominant source of anthropogenic Os in Japan.

Estimated MSWI emissions for Japan are several orders of magnitude higher than global natural Os inputs from atmospheric deposition, of 1 pg Os/m^2/yr [82], and continental erosion, of ~810 pg Os/m^2/yr [27], suggesting human activity in highly populated industrialised countries is having a significant impact on the local environment. Considering the large uncertainties associated with Os inventories calculated here, future work is needed to determine the exact composition of Japanese MSWI fly ash, in a similar manner to Funari *et al.*[23], and the differences between incinerator sizes if Os emission inventories developed in this study are to be used to accurately estimate the production of anthropogenic Os from Japan. Furthermore, estimates of Os emissions and their corresponding isotopic composition is needed for other anthropogenic sources, such as oil refineries, to ascertain their potential influence on the Os cycle.

If we assume that all volatile Os accumulates in precipitation after emission this would result in precipitation with a respective Os concentration of $\boxed{26^{+38}_{-18}}$ fg/g and $\boxed{6^{+10}_{-5}}$ ag/g for MSWI and vehicle exhaust, using a precipitation rate of 3.7 x 10^{17} g/yr for Japan[83]. The average estimate for precipitation concentration resulting from MSWI emissions is similar to measured precipitation in Asia of 23 ± 1 fg/g [7] suggesting the incineration of municipal waste may be the dominant source of anthropogenic Os to the Asian hydrological cycle. If we extrapolate across the global population, assuming these are industrialised regions that process solid waste via incineration, this results in a global emission of $\boxed{606^{+894}_{-418}}$ kg of anthropogenic Os to the atmosphere. The incineration of municipal waste therefore plays a significant role in the contribution of anthropogenic Os to the global Os cycle after the refining of PGE ores.

Supporting Information

Tables S1 and S2 show Re-Os abundance and isotope data for macroalgae from Tokyo Bay and the RMKB macroalgae standard, respectively. Fig. S1 and S2 respectively display population density for the Kanto Region and an Os emission inventory for Japan. Text S1 describes the results of an ANOVA test between the macroalgae species.

Acknowledgements

A.D. Sproson and D. Selby are indebted to G. Nowell, C.J. Ottley and Antonia Hoffman for technical support at Durham University. A.D. Sproson would like to thank the Japan Society for the Promotion of Science (JSPS) for funding this research through their Summer Program (SP15111) and Postdoctoral (PE17712) fellowships. D. Selby acknowledges the TOTAL Endowment Fund and Dida Scholarship of CUG Wuhan. We would also like to thank T. Fukui for guidance and access to the EAGrid2010 database and three anonymous reviewers for greatly improving this study.

Reference

1. Peucker-Ehrenbrink, B.; Ravizza, G., The marine osmium isotope record. *Terra Nova* **2000,** *12* (5), 205-219.

2. Peucker-Ehrenbrink, B.; Ravizza, G., Chapter 8 - Osmium Isotope Stratigraphy. In *The Geologic Time Scale*, Elsevier: Boston, 2012; pp 145-166.
3. Rauch, S.; Hemond, H. F.; Peucker-Ehrenbrink, B.; Ek, K. H.; Morrison, G. M., Platinum Group Element Concentrations and Osmium Isotopic Composition in Urban Airborne Particles from Boston, Massachusetts. *Environmental Science & Technology* **2005,** *39* (24), 9464-9470.
4. Rauch, S.; Peucker-Ehrenbrink, B.; Kylander, M. E.; Weiss, D. J.; Martinez-Cortizas, A.; Heslop, D.; Olid, C.; Mighall, T. M.; Hemond, H. F., Anthropogenic Forcings on the Surficial Osmium Cycle. *Environmental Science & Technology* **2010,** *44* (3), 881-887.
5. Sen, I. S.; Peucker-Ehrenbrink, B., Anthropogenic Disturbance of Element Cycles at the Earth's Surface. *Environmental Science & Technology* **2012,** *46* (16), 8601-8609.
6. Prouty, N. G.; Roark, E. B.; Koenig, A. E.; Demopoulos, A. W. J.; Batista, F. C.; Kocar, B. D.; Selby, D.; McCarthy, M. D.; Mienis, F.; Ross, S. W., Deep-sea coral record of human impact on watershed quality in the Mississippi River Basin. *Global Biogeochemical Cycles* **2014,** *28* (1), 29-43.
7. Chen, C.; Sedwick, P. N.; Sharma, M., Anthropogenic osmium in rain and snow reveals global-scale atmospheric contamination. *Proceedings of the National Academy of Sciences* **2009,** *106* (19), 7724-7728.
8. Lambert, D. D.; Foster, J. G.; Frick, L. R.; Hoatson, D. M.; Purvis, A., Application of the Re-Os isotopic system to the study of Precambrian magmatic sulfide deposits of Western Australia. *Australian Journal of Earth Sciences* **1998,** *45* (2), 265-284.
9. Walker, R.; Morgan, J.; Horan, M.; Czamanske, G.; Krogstad, E.; Fedorenko, V.; Kunilov, V., Re-Os isotopic evidence for an enriched-mantle source for the Noril'sk-type, ore-bearing intrusions, Siberia. *Geochimica et Cosmochimica Acta* **1994,** *58* (19), 4179-4197.
10. Morgan, J. W.; Walker, R. J.; Horan, M. F.; Beary, E. S.; Naldrett, A. J., 190Pt-186Os and 187Re-187Os systematics of the Sudbury Igneous Complex, Ontario. *Geochimica et Cosmochimica Acta* **2002,** *66* (2), 273-290.
11. McCandless, T.; Ruiz, J., Osmium isotopes and crustal sources for platinum-group mineralization in the Bushveld Complex, South Africa. *Geology* **1991,** *19* (12), 1225-1228.
12. Walker, R. J.; Prichard, H. M.; Ishiwatari, A.; Pimentel, M., The osmium isotopic composition of convecting upper mantle deduced from ophiolite chromites. *Geochimica et Cosmochimica Acta* **2002,** *66* (2), 329-345.
13. Finlay, A. J.; Selby, D.; Osborne, M. J., Re-Os geochronology and fingerprinting of United Kingdom Atlantic margin oil: Temporal implications for regional petroleum systems. *Geology* **2011,** *39* (5), 475-478.
14. Selby, D.; Creaser, R. A., Direct radiometric dating of hydrocarbon deposits using rhenium-osmium isotopes. *Science* **2005,** *308* (5726), 1293-1295.
15. Selby, D.; Creaser, R. A.; Dewing, K.; Fowler, M., Evaluation of bitumen as a 187Re–187Os geochronometer for hydrocarbon maturation and migration: a test case from the Polaris MVT deposit, Canada. *Earth and Planetary Science Letters* **2005,** *235* (1-2), 1-15.
16. Selby, D.; Creaser, R. A.; Fowler, M. G., Re–Os elemental and isotopic systematics in crude oils. *Geochimica et Cosmochimica Acta* **2007,** *71* (2), 378-386.
17. Turekian, K. K.; Sharma, M.; Gordon, G. W., The behavior of natural and anthropogenic osmium in the Hudson River–Long Island Sound estuarine system. *Geochimica et Cosmochimica Acta* **2007,** *71* (17), 4135-4140.

18. Williams, G.; Marcantonio, F.; Turekian, K. K., The behavior of natural and anthropogenic osmium in Long Island Sound, an urban estuary in the eastern US. *Earth and planetary science letters* **1997,** *148* (1-2), 341-347.
19. Esser, B. K.; Turekian, K. K., Anthropogenic osmium in coastal deposits. *Environmental science & technology* **1993,** *27* (13), 2719-2724.
20. Ravizza, G.; Bothner, M. H., Osmium isotopes and silver as tracers of anthropogenic metals in sediments from Massachusetts and Cape Cod bays. *Geochimica et Cosmochimica Acta* **1996,** *60* (15), 2753-2763.
21. Rauch, S.; Hemond, H. F.; Peucker-Ehrenbrink, B., Recent changes in platinum group element concentrations and osmium isotopic composition in sediments from an urban lake. *Environmental science & technology* **2004,** *38* (2), 396-402.
22. Helz, G. R.; Adelson, J. M.; Miller, C. V.; Cornwell, J. C.; Hill, J. M.; Horan, M.; Walker, R. J., Osmium isotopes demonstrate distal transport of contaminated sediments in Chesapeake Bay. *Environmental science & technology* **2000,** *34* (12), 2528-2534.
23. Funari, V.; Meisel, T.; Braga, R., The potential impact of municipal solid waste incinerators ashes on the anthropogenic osmium budget. *Science of The Total Environment* **2016,** *541*, 1549-1555.
24. Widory, D.; Vautour, G.; Poirier, A., Atmospheric dispersion of trace metals between two smelters: An approach coupling lead, strontium and osmium isotopes from bioindicators. *Ecological Indicators* **2018,** *84*, 497-506.
25. Gogot, J.; Poirier, A.; Boullemant, A., Osmium isotopic tracing of atmospheric emissions from an aluminum smelter. *Comptes Rendus Geoscience* **2015,** *347* (5-6), 277-283.
26. Rodushkin, I.; Engström, E.; Sörlin, D.; Pontér, C.; Baxter, D. C., Osmium in environmental samples from Northeast Sweden. Part II. Identification of anthropogenic sources. *Science of the total environment* **2007,** *386* (1-3), 159-168.
27. Poirier, A.; Gariépy, C., Isotopic signature and impact of car catalysts on the anthropogenic osmium budget. *Environmental science & technology* **2005,** *39* (12), 4431-4434.
28. Qi, L.; Zhou, M.-F.; Zhao, Z.; Hu, J.; Huang, Y., The characteristics of automobile catalyst-derived platinum group elements in road dusts and roadside soils: a case study in the Pearl River Delta region, South China. *Environmental Earth Sciences* **2011,** *64* (6), 1683-1692.
29. Levasseur, S.; Birck, J.-L.; Allegre, C., The osmium riverine flux and the oceanic mass balance of osmium. *Earth and Planetary Science Letters* **1999,** *174* (1-2), 7-23.
30. Gannoun, A.; Burton, K. W.; Vigier, N.; Gíslason, S. R.; Rogers, N.; Mokadem, F.; Sigfússon, B., The influence of weathering process on riverine osmium isotopes in a basaltic terrain. *Earth and Planetary Science Letters* **2006,** *243* (3), 732-748.
31. Levasseur, S.; Birck, J.-L.; Allègre, C. J., Direct measurement of femtomoles of osmium and the 187Os/186Os ratio in seawater. *Science* **1998,** *282* (5387), 272-274.
32. Sharma, M.; Papanastassiou, D.; Wasserburg, G., The concentration and isotopic composition of osmium in the oceans. *Geochimica et Cosmochimica Acta* **1997,** *61* (16), 3287-3299.
33. Gannoun, A.; Burton, K. W., High precision osmium elemental and isotope measurements of North Atlantic seawater. *Journal of Analytical Atomic Spectrometry* **2014,** *29* (12), 2330-2342.

34. Martin, C. E.; Peucker-Ehrenbrink, B.; Brunskill, G.; Szymczak, R., Osmium isotope geochemistry of a tropical estuary. *Geochimica et Cosmochimica Acta* **2001,** *65* (19), 3193-3200.
35. Woodhouse, O.; Ravizza, G.; Falkner, K. K.; Statham, P.; Peucker-Ehrenbrink, B., Osmium in seawater: vertical profiles of concentration and isotopic composition in the eastern Pacific Ocean. *Earth and Planetary Science Letters* **1999,** *173* (3), 223-233.
36. Sharma, M.; Wasserburg, G., Osmium in the rivers. *Geochimica et Cosmochimica Acta* **1997,** *61* (24), 5411-5416.
37. Peucker-Ehrenbrink, B.; Jahn, B.-m., Rhenium-osmium isotope systematics and platinum group element concentrations: Loess and the upper continental crust. *Geochemistry, Geophysics, Geosystems* **2001,** *2* (10).
38. Walker, R. J.; Horan, M. F.; Morgan, J. W.; Becker, H.; Grossman, J. N.; Rubin, A. E., Comparative 187Re-187Os systematics of chondrites: Implications regarding early solar system processes. *Geochimica et Cosmochimica Acta* **2002,** *66* (23), 4187-4201.
39. Krähenbühl, U.; Geissbühler, M.; Bühler, F.; Eberhardt, P.; Finnegan, D. L., Osmium isotopes in the aerosols of the mantle volcano Mauna Loa. *Earth and planetary science letters* **1992,** *110* (1-4), 95-98.
40. Yudovskaya, M. A.; Tessalina, S.; Distler, V. V.; Chaplygin, I. V.; Chugaev, A. V.; Dikov, Y. P., Behavior of highly-siderophile elements during magma degassing: A case study at the Kudryavy volcano. *Chemical Geology* **2008,** *248* (3-4), 318-341.
41. Zheng, G.; Suzuki, K.; Kuno, A.; Mastuo, M.; Takano, B.; Shimizu, H., Osmium geochemistry of modern estuarine sediments from the Tama and Yasaka rivers in Japan. *Applied geochemistry* **2014,** *40*, 82-88.
42. Jackson, M. T.; Prichard, H. M.; Sampson, J., Platinum-group elements in sewage sludge and incinerator ash in the United Kingdom: Assessment of PGE sources and mobility in cities. *Science of the total environment* **2010,** *408* (6), 1276-1285.
43. Rodushkin, I.; Engström, E.; Sörlin, D.; Pontèr, C.; Baxter, D. C., Osmium in environmental samples from Northeast Sweden: Part I. Evaluation of background status. *Science of the total environment* **2007,** *386* (1-3), 145-158.
44. Sproson, A. D.; Selby, D.; Gannoun, A.; Burton, K. W.; Dellinger, M.; Lloyd, J. M., Tracing the Impact of Coastal Water Geochemistry on the Re-Os Systematics of Macroalgae: Insights From the Basaltic Terrain of Iceland. *Journal of Geophysical Research: Biogeosciences* **2018,** *123* (9), 2791-2806.
45. Rooney, A. D.; Selby, D.; Lloyd, J. M.; Roberts, D. H.; Lückge, A.; Sageman, B. B.; Prouty, N. G., Tracking millennial-scale Holocene glacial advance and retreat using osmium isotopes: Insights from the Greenland ice sheet. *Quaternary Science Reviews* **2016,** *138*, 49-61.
46. Ownsworth, E.; Selby, D.; Ottley, C. J.; Unsworth, E.; Raab, A.; Feldmann, J.; Sproson, A. D.; Kuroda, J.; Faidutti, C.; Bücker, P., Tracing the natural and anthropogenic influence on the trace elemental chemistry of estuarine macroalgae and the implications for human consumption. *Science of the Total Environment* **2019,** *685*, 259-272.
47. Racionero-Gómez, B.; Sproson, A.; Selby, D.; Gannoun, A.; Gröcke, D.; Greenwell, H.; Burton, K. W., Osmium uptake, distribution, and 187Os/188Os and 187Re/188Os compositions in Phaeophyceae macroalgae, Fucus vesiculosus: Implications for determining the 187Os/188Os composition of seawater. *Geochimica et Cosmochimica Acta* **2017,** *199*, 48-57.

48. Peucker-Ehrenbrink, B.; Sharma, M.; Reisberg, L., Recommendations for Analysis of Dissolved Osmium in Seawater: Dissolved Osmium Isotope Analysis; Montreal, Canada, 24 June 2012. *Eos, Transactions American Geophysical Union* **2013,** *94* (7), 73-73.
49. Connan, S.; Stengel, D. B., Impacts of ambient salinity and copper on brown algae: 1. Interactive effects on photosynthesis, growth, and copper accumulation. *Aquatic Toxicology* **2011,** *104* (1), 94-107.
50. Ho, Y. B., Ulva lactuca as bioindicator of metal contamination in intertidal waters in Hong Kong. *Hydrobiologia* **1990,** *203* (1), 73-81.
51. Rainbow, P. S., Biomonitoring of heavy metal availability in the marine environment. *Marine Pollution Bulletin* **1995,** *31* (4), 183-192.
52. Racionero-Gómez, B.; Sproson, A.; Selby, D.; Gröcke, D.; Redden, H.; Greenwell, H., Rhenium uptake and distribution in phaeophyceae macroalgae, Fucus vesiculosus. *Royal Society open science* **2016,** *3* (5), 160161.
53. Pan, S.; Kadokami, K.; Li, X.; Duong, H. T.; Horiguchi, T., Target and screening analysis of 940 micro-pollutants in sediments in Tokyo Bay, Japan. *Chemosphere* **2014,** *99*, 109-116.
54. Sakurai, T.; Serizawa, S.; Kobayashi, J.; Kodama, K.; Lee, J.-H.; Maki, H.; Zushi, Y.; Sevilla-Nastor, J. B.; Imaizumi, Y.; Suzuki, N., Temporal trends for inflow of perfluorooctanesulfonate (PFOS) and perfluorooctanoate (PFOA) to Tokyo Bay, Japan, estimated by a receptor-oriented approach. *Science of the Total Environment* **2016,** *539*, 277-285.
55. TBEIC Tokyo Bay Environmental Information Center, Industry surrounding Tokyo Bay. <https://www.tbeic.go.jp/kankyo/sangyo.asp>.
56. Selby, D.; Creaser, R. A., Re-Os geochronology and systematics in molybdenite from the Endako porphyry molybdenum deposit, British Columbia, Canada. *Economic Geology* **2001,** *96* (1), 197-204.
57. Creaser, R. A.; Sannigrahi, P.; Chacko, T.; Selby, D., Further evaluation of the Re-Os geochronometer in organic-rich sedimentary rocks: A test of hydrocarbon maturation effects in the Exshaw Formation, Western Canada Sedimentary Basin. *Geochimica et Cosmochimica Acta* **2002,** *66* (19), 3441-3452.
58. Birck, J. L.; Barman, M. R.; Capmas, F., Re-Os isotopic measurements at the femtomole level in natural samples. *Geostandards newsletter* **1997,** *21* (1), 19-27.
59. Cohen, A. S.; Waters, F. G., Separation of osmium from geological materials by solvent extraction for analysis by thermal ionisation mass spectrometry. *Analytica Chimica Acta* **1996,** *332* (2-3), 269-275.
60. Cumming, V. M.; Poulton, S. W.; Rooney, A. D.; Selby, D., Anoxia in the terrestrial environment during the late Mesoproterozoic. *Geology* **2013,** *41* (5), 583-586.
61. Creaser, R.; Papanastassiou, D.; Wasserburg, G., Negative thermal ion mass spectrometry of osmium, rhenium and iridium. *Geochimica et Cosmochimica Acta* **1991,** *55* (1), 397-401.
62. Völkening, J.; Walczyk, T.; Heumann, K. G., Osmium isotope ratio determinations by negative thermal ionization mass spectrometry. *International Journal of Mass Spectrometry and Ion Processes* **1991,** *105* (2), 147-159.
63. Nowell, G. M.; Pearson, D. G.; Parman, S. W.; Luguet, A.; Hanski, E., Precise and accurate 186Os/188Os and 187Os/188Os measurements by Multi-collector Plasma Ionisation Mass Spectrometry, part II: Laser ablation and its application to single-grain Pt–Os and Re–Os geochronology. *Chemical Geology* **2008,** *248* (3), 394-426.

64. Fukui, T.; Kokuryo, K.; Baba, T.; Kannari, A., Updating EAGrid2000-Japan emissions inventory based on the recent emission trends. *Journal of Japan Society for Atmospheric Environment* **2014,** *49* (2), 117-125.
65. Oda, T.; Maksyutov, S.; Andres, R. J., The Open-source Data Inventory for Anthropogenic CO2, version 2016 (ODIAC2016): a global monthly fossil fuel CO2 gridded emissions data product for tracer transport simulations and surface flux inversions. *Earth Syst. Sci. Data* **2018,** *10* (1), 87-107.
66. JAMA Motor Vehicle Statistics of Japan. <http://www.jama-english.jp>.
67. Andres, R. J.; Boden, T. A.; Higdon, D. M., Gridded uncertainty in fossil fuel carbon dioxide emission maps, a CDIAC example. *Atmos. Chem. Phys.* **2016,** *16* (23), 14979-14995.
68. Oda, T.; Bun, R.; Kinakh, V.; Topylko, P.; Halushchak, M.; Marland, G.; Lauvaux, T.; Jonas, M.; Maksyutov, S.; Nahorski, Z.; Lesiv, M.; Danylo, O.; Horabik-Pyzel, J., Errors and uncertainties in a gridded carbon dioxide emissions inventory. *Mitigation and Adaptation Strategies for Global Change* **2019,** *24* (6), 1007-1050.
69. Colodner, D.; Sachs, J.; Ravizza, G.; Turekian, K.; Edmond, J.; Boyle, E., The geochemical cycle of rhenium: a reconnaissance. *Earth and Planetary Science Letters* **1993,** *117* (1-2), 205-221.
70. Sharma, M.; Balakrishna, K.; Hofmann, A.; Shankar, R., The transport of osmium and strontium isotopes through a tropical estuary. *Geochimica et Cosmochimica Acta* **2007,** *71* (20), 4856-4867.
71. Levasseur, S.; Rachold, V.; Birck, J.-L.; Allegre, C., Osmium behavior in estuaries: the Lena River example. *Earth and Planetary Science Letters* **2000,** *177* (3-4), 227-235.
72. Fujiwara, T.; Yamada, Y., Inflow of oceanic water into Tokyo Bay and generation of a subsurface hypoxic water mass. *Journal of Geophysical Research: Oceans* **2002,** *107* (C5), 13-1-13-9.
73. Sugiyama, Y.; Sugai, T.; Imura, R.; Mizuno, K.; Endo, H.; Shimokawa, K.; Yamazaki, H., Neotectonic Map. 1: 500,000 Neotectonic map, sheet 8, Tokyo. Geological Survey of Japan: 1997.
74. Okada, T.; Nakayama, K.; Takao, T.; Furukawa, K., Influence of freshwater input and bay reclamation on long-term changes in seawater residence times in Tokyo Bay, Japan. *Hydrological Processes* **2011,** *25* (17), 2694-2702.
75. Takahashi, M.; Yanagisawa, Y.; Hayashi, H.; Kasahara, K.; Ikawa, T.; Kawanaka, T.; Suda, S. In *Miocene subsurface half-grabens in the Kanto Plain, central Japan*, Proceedings of International Workshop on Strong Ground Motion Prediction and Earthquake Tectonics in Urban Areas, Tokyo, 2005; pp 65-74.
76. Zheng, G.; Suzuki, K.; Miyata, Y.; Shimizu, H., Osmium concentrations and 187Os/188Os ratios of three sediment reference materials. *Geochemical Journal* **2012,** *46* (2), 143-149.
77. Kubo, S., The uplands and lowlands of Tokyo: A geomorphological outline. *Geographical review of Japan, Series B.* **1990,** *63* (1), 73-87.
78. Suzuki, K.; Tatsumi, Y., Osmium concentrations and 187Os/188Os ratios of GSJ reference samples, JB-1a, JA-2 and JP-1. *Geochemical Journal* **2001,** *35* (3), 207-210.
79. Cumming, V. M.; Selby, D.; Lillis, P. G., Re–Os geochronology of the lacustrine Green River Formation: Insights into direct depositional dating of lacustrine successions, Re–Os systematics and paleocontinental weathering. *Earth and Planetary Science Letters* **2012,** *359*, 194-205.

80. Harris, N. B.; Mnich, C. A.; Selby, D.; Korn, D., Minor and trace element and Re–Os chemistry of the Upper Devonian Woodford Shale, Permian Basin, west Texas: Insights into metal abundance and basin processes. *Chemical Geology* **2013,** *356*, 76-93.
81. Smith, S.; Yanagi, T., NP Budgets for three Japanese Bays. LOICZ e Biogeochemical Modelling Node. 1997.
82. Williams, G. A.; Turekian, K. K., Atmospheric supply of osmium to the oceans. *Geochimica et cosmochimica acta* **2002,** *66* (21), 3789-3791.
83. Berner, E. K.; Berner, R. A., *Global environment: water, air, and geochemical cycles*. Princeton University Press: 2012.